Ukrainian Journal of Physical Optics
ISSUE 2
2026

IN-DEPTH NUMERICAL EVALUATION AND PERFORMANCE OPTIMIZATION OF CMTS PHOTODETECTOR

S. YASIN [1]*, Z. ABU WAAR [2], S. CHRISTOPOULOS [3], M. MOUSTAFA [4]

[1] College of Integrative Studies, Abdullah Al Salem University, Khaldiya, Kuwait
[2] Department of Physics, College of Science, The University of Jordan, Amman, 11942, Jordan
[3] Sorbonne University Abu Dhabi, SAFIR, Novel Materials Development Laboratory, Abu Dhabi, United Arab Emirates
[4] Department of Physics, School of Sciences and Engineering, The American University in Cairo, New Cairo 11835, Egypt.
* Corresponding Author: shadi.yasin@aasu.edu.kw

Received: 29.01.2026

Abstract. Photodetectors are essential elements in a wide range of technological fields, especially for advanced photosensing applications. This study presents a detailed numerical assessment and optimization of the performance of Copper Manganese Tin Sulfide (CMTS) layers, with particular focus on the absorber layer in a photodetector device. The investigation focuses on the influence of various design parameters, with an emphasis on maximizing the efficiency and functionality of the Fluorine-doped Tin Oxide (FTO)/CMTS/Au structure. A comprehensive numerical analysis of the physical properties of the CMTS absorber layer identifies, within the studied range, the optimal thickness, bandgap, doping density, and electron-hole mobility for enhanced photodetector performance at 1000 nm, 1.3 eV, 1×10^{14} cm^{-3}, and 28 cm^2/Vs, respectively. Additionally, the influence of the incident light wavelength on photodetector behaviour is explored. The results indicate that the device performs optimally with an incident light wavelength of 800 nm. Under these optimized values and conditions, the photodetector achieves a responsivity of 0.56 A/W and a detectivity of 5.17×10^{13} Jones. These results demonstrate that the proposed device offers a promising pathway toward cost-effective, easily fabricated, and robust photodetectors, establishing it as a highly promising material for future photosensing technology.

Keywords: photodetector, copper-manganese-tin sulfide, responsivity, detectivity, solar cell capacitance simulator
UDC: 535.2
DOI: 10.3116/16091833/Ukr.J.Phys.Opt.2026.02058

1. Introduction

Photodetectors are key components in modern optoelectronic systems, enabling the efficient conversion of optical signals into electrical responses for a wide range of applications. Their role is fundamental in areas such as telecommunications, environmental monitoring, medical imaging, and even space exploration [1-2]. As light-sensitive devices, photodetectors are essential for capturing and analyzing light information across the visible spectrum to the far-infrared. The growing demand for faster, more efficient, and compact photodetectors has spurred innovation in materials science, leading to the development of new types with improved performance [3-4]. Several key parameters are used to evaluate photodetector performance. One of these is quantum efficiency (QE), which quantifies the proportion of incoming photons that successfully produce an electrical signal. Another vital parameter is the noise equivalent power (NEP), which represents the minimum detectable light intensity of the device. In addition, responsivity (R) measures the photodetector's efficiency in converting optical power into an electrical signal, and detectivity (D) gauges the device's sensitivity to weak signals, highlighting its ability to detect low light levels [5-7].

Photodetector materials are at the forefront of optical sensing technologies, with their evolution driven by the need for high efficiency, low cost, and versatile performance across a wide range of wavelengths. To date, most commercial photodetectors rely on silicon- and inorganic-materials-based semiconductors. These materials offer reliable performance but are hampered by complex, expensive manufacturing processes that often require vacuum conditions, making large-scale production challenging [8]. In contrast, organic materials such as polymers and quantum dots have been considered potential alternatives due to their solution-based fabrication methods, which are cost-effective and scalable. Additionally, they can detect a wide range of wavelengths, from visible to near-infrared. However, their performance is often limited by low light absorption and inferior electrical characteristics, making them less suitable for high-performance applications [8]. Alternatively, perovskite materials have attracted significant attention for their outstanding properties, including high sensitivity, tunable band gaps, and low-cost, solution-processable fabrication methods. These materials have proven effective in a variety of optoelectronic devices, such as solar cells, light-emitting diodes, and photodetectors, and are particularly attractive for applications requiring high efficiency [9-13]. Several studies have reported on the development and improvement of photodetectors' performance through utilizing perovskite materials. Geng et al. developed a heterojunction photodetector by integrating MAPbBr3 organic-inorganic perovskite single crystals onto a Si wafer. This photodetector exhibited a detectable spectrum ranging from 405 to 1064 nm, offering fast response times and high stability [14]. Zhao et. al. developed a large-area perovskite-filled membrane X-ray detector on a flexible substrate [15]. The resulting photodetector exhibited a sensitivity of $8696\pm228\ \mu C\times Gy_{air}^{-1}\times cm^{-2}$ within an applied electric field range of 0.05 V μm^{-1}. Dong et al. fabricated $CsPbBr_3$ perovskite nanocrystals on a Si substrate using centrifugal casting and incorporated Au interdigital electrode pairs. The obtained photodetector demonstrated a responsivity and detectivity of 10.04 mAW^{-1} and 4.56×10^{8} Jones, respectively [16].

Recently, multinary chalcogenide semiconductor materials showed a remarkable potential as light harvesters in optoelectronic devices. Their exceptional physical and chemical properties, such as high absorption coefficients across a broad range of the solar spectrum, tunable band gaps, remarkable stability, and excellent power conversion efficiency, make them leading candidates for the next generation of optoelectronic materials [17-18]. Common types of multinary chalcogenides, such as $Cu(In,Ga)Se_2$ (CIGS) and Cu_2ZnSnS_4 (CZTS), and their related compounds have been widely investigated and utilized in optoelectronic applications, such as solar cells and photodetectors [19]. Yılmaz et al. have fabricated a high-performance CIGS-based photodetector that demonstrated a responsivity of 4.44×10^{-1} A/W and a detectivity of 8.0×10^{7} Jones [20]. H. Wu et al. have investigated the impact of defects in a CZTS-based photodetector on optoelectrical processes and photoresponse. Optimal performance was achieved with responsivity and detectivity values of 220 mA/W and 2.7×10^{10} Jones, respectively. However, among several outstanding multinary chalcogenide semiconductor materials that have emerged as absorber materials, Copper Manganese Tin Sulfide (CMTS) has recently attracted significant attention in the field of optoelectronic device research due to its promising potential [21]. Although CMTS is a compound semiconductor with a chalcogenide (sulfide) structure like other well-known materials, such as CIGS and CdTe, it stands out for its unique properties. Among these

features are a tunable band gap spanning 1.1 to 1.5 eV, a high absorption coefficient (>10^4 cm^{-1}), excellent material stability, low cost, and an environmentally friendly composition [22-24]. These characteristics make CMTS a promising candidate for next-generation thin-film photovoltaic and optoelectronic applications [24]. The impressive properties of CMTS have been highlighted in several studies, primarily focusing on solar cell devices. However, to the best of our knowledge, no studies have yet explored its potential in photodetector applications.

Herein, we report an in-depth numerical analysis highlighting CMTS as a promising material for next-generation photodetector applications. A metal–semiconductor–metal (MSM) structure was selected for the device design due to its advantages, including high sensitivity, low dark current, and straightforward integration into electronic circuits [25-26]. The performance of the Fluorine-doped Tin Oxide (FTO)/CMTS/Au photodetector was evaluated using the one-dimensional Solar Cell Capacitance Simulator (SCAPS-1D) [27]. To achieve optimal device performance, key parameters, including the absorber layer thickness, defect density, and electron-hole mobilities in CMTS, were systematically varied. Additionally, the influence of incident wavelength on the device characteristics was thoroughly investigated.

2.2. Research methodology and photodetector structure

Computational simulations are fundamental to advancing and fine-tuning optoelectronic technologies, providing invaluable insights into device performance before physical prototypes are produced. These simulations are essential for optimizing designs and predicting operational efficiency under various conditions. Among the diverse array of simulation tools available, SCAPS-1D stands out for its precision and reliability in modeling the behavior of optoelectronic devices. Several studies have demonstrated its ability to closely match experimental outcomes, solidifying SCAPS-1D as a trusted tool in this field [28-30]. SCAPS-1D works on solving three fundamental semiconductor equations: the Poisson equation, and continuity equations for electrons and holes, simultaneously. It is characterized by its ability to operate over a well-defined, wide range of input parameters, such as operating temperature, resistance, shunt resistances, illumination power, and spectral wavelength. It incorporates physical parameters for each layer in the modeled device, including the energy band gap, electron affinity, and doping density [31]. As a result, various optoelectronic output parameters, such as photocurrent density (Jph), voltage (V), and total external QE, can be obtained.

To evaluate and track the performance of the modelled photodetector under several conditions, key parameters such as the responsivity (R) and detectivity (D) were considered, as defined in equations [26, 32-34]:

$$R = \frac{I_{ph}}{P_i S} \tag{1}$$

$$D = \sqrt{\frac{R^2 S}{2qI_d}} \tag{2}$$

where Iph and Id are the photocurrent and dark current, respectively. P_i is the intensity of the incident spectrum, assumed at 1000 W/m^2 unless otherwise specified, S is the effective area of

the photodetector, and q is the electric charge of the charge carriers ($|q_e|$=1.6×10^{-19} C). As shown in Eq. (2), the detectivity is inversely proportional to the dark current. In this study, the dark current is identified at a bias voltage of -0.5 V (though this value is not explicitly shown).

Figure 1 illustrates the structure of the modeled photodetector (Fig. 1a) along with its corresponding energy band alignment obtained from SCAPS simulation (Fig. 1b). The device uses an MSM configuration, specifically FTO/CMTS/Au, where CMTS serves as the core material. All initial input parameters for the layers are provided in Table 1, which were sourced from recent research studies [7, 35-36]. As depicted in the energy band diagram, the CMTS material does not exhibit a uniform energy band across its thickness. This variation is attributed to band bending, which occurs due to an external electric field or an interface with another material, typically at the semiconductor-metal junction [37]. In the present study, all simulations were systematically conducted using SCAPS-1D at an operating temperature of 300 K and solar spectrum intensity of 1000 W/m^2. Initially, the influence of CMTS layer thickness on the photodetection properties was examined to determine the optimal thickness. Subsequently, the effects of bandgap, doping density, and electron-hole mobility density were investigated and discussed. Finally, to further optimize photodetector performance, the impact of solar spectrum wavelength was analyzed.

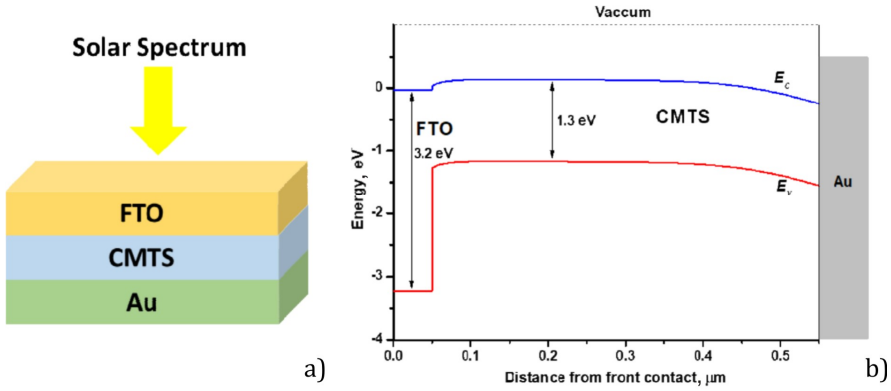

Fig. 1. Device structure of modeled CMTS-based photodetector (a) and its energy band structure (b).

Table 1. Initial input parameters for the layers [7, 35-36].

Parameters	**FTO**	**CMTS**
Thickness (nm)	50	500 (varied)
Band gap (eV)	3.2	1.3 (varied)
Electron affinity (eV)	4.4	4.35
Dielectric Permittivity	9.0	9
CB effective density of states (cm^{-3})	2.2×10^{18}	3.1×10^{18}
VB effective density of states (cm^{-3})	1.8×10^{18}	1.8×10^{19}
Electron thermal velocity (cm/s)	1×10^7	1×10^7
Hole thermal velocity (cm/s)	1×10^7	1×10^7
Electron mobility (cm^2/V s)	20	0.16 (varied)
Hole mobility (cm^2/V s)	10	0.16 (varied)
Donor doping concentration (cm^{-3})	1×10^{19}	0
Acceptor doping concentration (cm^{-3})	0	1×10^{16} (varied)
Defect density (cm^{-3})	1×10^{14}	1×10^{14}

3. Results and discussion

The absorber layer is the core component of a photodetector, serving as the photon harvester. Optimizing its physical parameters, particularly its thickness, is vital for maximizing the photodetection response. While greater thickness generally increases absorption, this improvement is limited, as excessive thickness can degrade performance due to an increased recombination rate [38]. We investigated the impact of CMTS thickness on photodetection (Fig. 2), varying it from 100 nm to 1000 nm while keeping other parameters constant. The results clearly show a positive correlation (Fig. 2a). Specifically, the photocurrent increased from 16.11 mA/cm^{-3} to 32.69 mA/cm^{-3} as the thickness increased from 100 nm to 1000 nm (Fig. 2b). Notably, the photocurrent began to saturate above 700 nm, stabilizing at 32 mA/cm^{-3}. This positive effect was mirrored in QE (Fig. 2 c). In the optimal spectrum range of 390 nm – 600 nm, the QE rose from 68.3% at 100 nm thickness to a maximum of 99.89% at 1000 nm. This directly confirms that increasing the absorber thickness enhances absorption of the solar spectrum and, consequently, the charge-carrier generation rate.

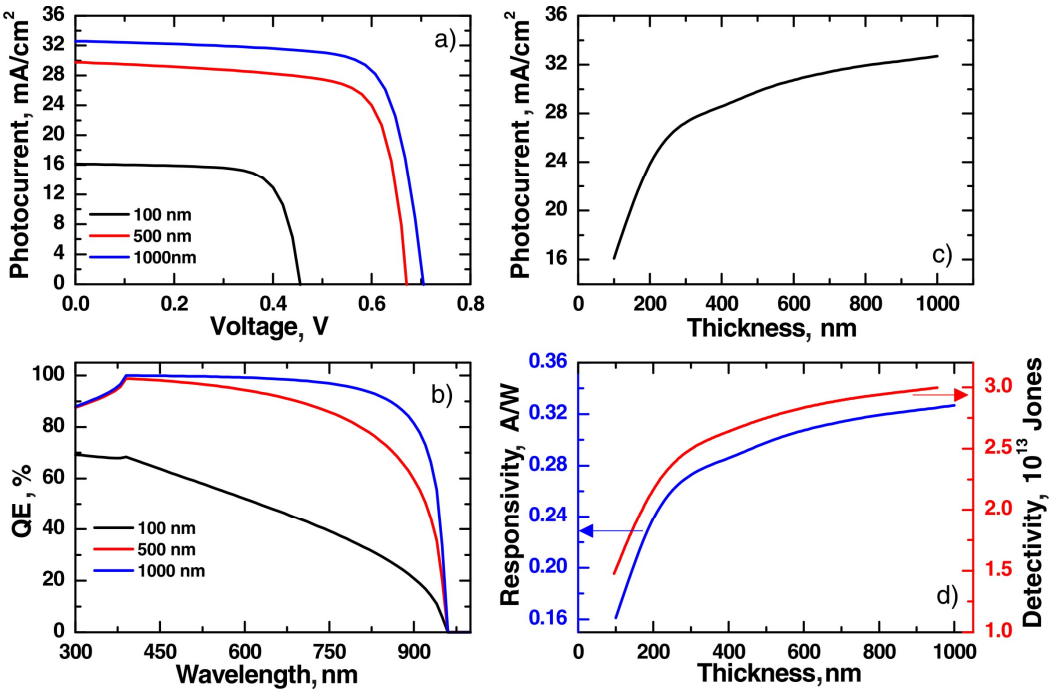

Fig. 2. Impact of the CMTS thickness: (a) Photocurrent–voltage characteristics for various thicknesses. (b) QE characteristics for various doping densities. (c) Effect of the thickness on the photocurrent (c). (d) Influence of the thickness on the photodetector's responsivity (left) and detectivity (right).

The influence of the absorber layer thickness on device sensitivity was systematically examined by evaluating responsivity and detectivity, as defined by Eq. (1) and (2), respectively. As illustrated in Fig. 2d, increasing the absorber thickness had a positive effect on both parameters. Responsivity increased from 0.16 A/W to 0.33 A/W as the thickness increased from 100 nm to 1000 nm. In parallel, the detectivity improved from 1.74×10^{13} Jones to 2.99×10^{13} Jones. These results demonstrate a marked improvement compared with those reported in the literature for analogous compounds such as CIGS and CZTS [25, 39]. However, the positive impact of the absorber thickness can be clarified as

follows. As the thickness of a photodetector's active layer increases, both its responsivity and detectivity generally improve because a thicker layer allows more incident spectrum intensity to be absorbed. When the thickness increases, a larger fraction of incident photons is absorbed within the material, leading to the generation of more electron–hole pairs. This enhances the device's quantum efficiency and results in a higher photocurrent for a given optical power, thereby increasing the responsivity. Similarly, detectivity, which depends on the signal-to-noise ratio, also tends to increase because the signal (photocurrent) rises faster than the noise current, provided that the dark current does not increase significantly with thickness. Furthermore, Fig. 2d reveals that responsivity and detectivity exhibit saturation behavior at high absorber thicknesses above 1000 nm. This finding aligns with the fact that responsivity and detectivity increase up to a point as thickness increases. If the active layer becomes too thick, photogenerated carriers may recombine before reaching the electrodes due to limited carrier diffusion lengths, reducing collection efficiency and slowing the detector's response time, thereby degrading its performance. In this study, we considered a 1000 nm CMTS thickness as optimal for the modelled photodetector, which in turn leads to high detectivity and responsivity and avoids a slow detector response time.

The doping density of the absorber layer is a key parameter that strongly impacts the performance of optoelectronic devices. To investigate its impact on our modeled photodetector, the CMTS doping density was varied from 1×10^{14} cm^{-3} to 1×10^{20} cm^{-3}. As illustrated in Fig. 3a and 3b, an increase in doping density markedly reduces the photocurrent, which drops from 34.19 mA/cm^2 at 1×10^{14} cm^{-3} to 26.87 mA/cm^2 at 1×10^{20} cm^{-3}. This negative impact is also mirrored in the quantum efficiency behavior. As

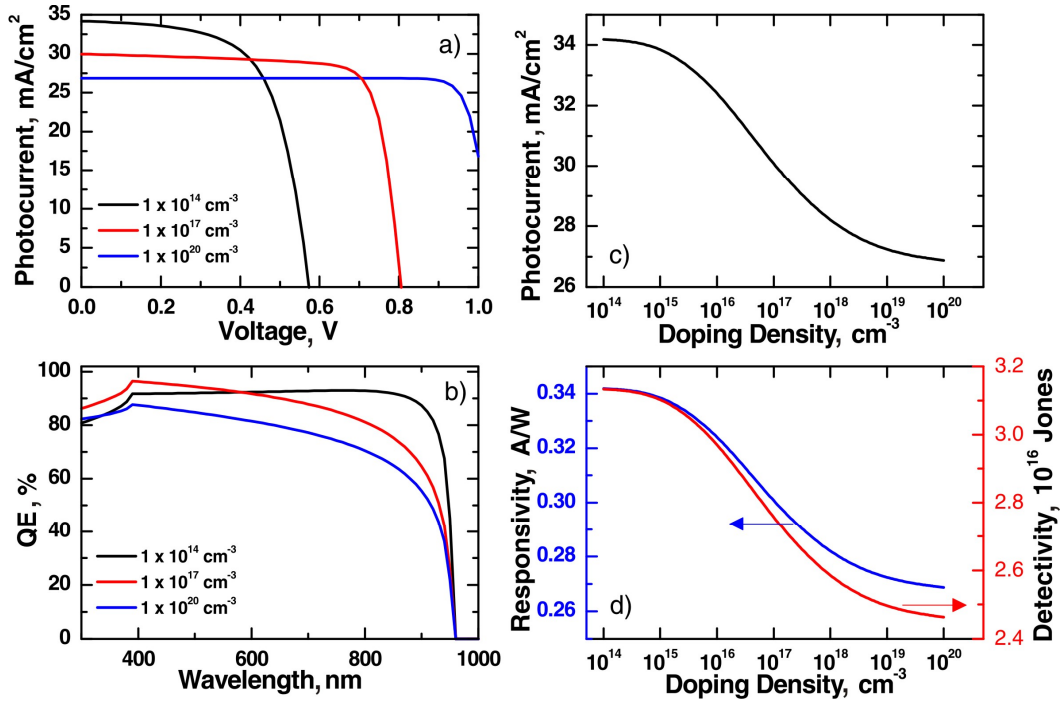

Fig. 3. Impact of the CMTS doping density: (a) Photocurrent–voltage characteristics for various doping densities. (b) QE characteristics for various doping densities. (c) Effect of the doping density on the photocurrent. (d) Influence of the doping density on the photodetector's responsivity (left) and detectivity (right).

shown in Fig. 3c, the QE varied by approximately 10% across the entire range of doping densities. The harsh negative impact of the increase in doping density in CMTS has clearly affected responsivity and detectivity. Responsivity decreased by about 0.07 A/W, while detectivity decreased by 21.4%.

A decrease in photodetector performance with increasing doping density has been observed in several studies [40-41] and can be attributed to several factors. Increasing doping density in a semiconductor (CMTS) reduces responsivity and detectivity by increasing carrier recombination and thereby shortening the carrier lifetime. This leads to lower carrier collection efficiency and higher dark current, which results in decreased overall performance. In this study, we consider the optimal doping density of 1×10^{14} cm^{-3}, at which the responsivity and detectivity reach their maximum values of 0.34 A/W and 3.13×10^{13} Jones, respectively.

The energy bandgap of the absorber layer is of paramount importance in the performance of a photodetector. It influences key factors like light absorption, photocurrent generation, and overall sensitivity. Figure 4 shows the change in the detectivity and responsivity with increasing the energy band gap of CMTS from 1.3 eV to 1.6 eV. Both performance parameters show a decline with increasing band gap energy. The detectivity and responsivity decrease from 2.99×10^{13} Jones and 0.33 A/W to 2.05×10^{13} Jones and 0.22 A/W, respectively, when the energy band gap increases from 1.3 eV to 1.6 eV. This trend can be attributed to the fact that a larger band gap requires more energy for electrons to jump from the valence band to the conduction band, meaning fewer electron-hole pairs are generated under the same incident light. This reduces the photocurrent, lowering responsivity. Additionally, a larger band gap tends to reduce the absorption of lower-energy photons, making the material less sensitive to a broader range of wavelengths. As a result, both light absorption efficiency and the device's overall performance decrease, thereby reducing detectivity.

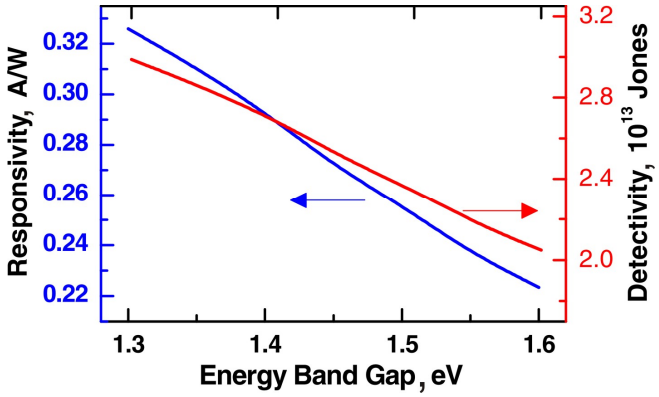

Fig. 4. Influence of the CMTS energy band gap variation on the photodetector's responsivity (left) and detectivity (right).

To further optimize the modeled CMTS-based photodetector and to explore the impact of another intrinsic property of the absorber layer, the effect of electron/hole mobility has been examined. The electron/hole mobility is the proportionality constant between the charge-carrier drift velocity and the applied electric field, reflecting the ease with which charge carriers move through the semiconductor lattice. The electron/hole mobility varied from 0.16 $cm^2/V\,s$ to 28 $cm^2/V\,s$, as shown in Fig. 5. Both responsivity and detectivity

displayed a tiny increase with increasing mobility from 0.6 $cm^2/V\,s$ to 4 $cm^2/V\,s$, followed by invariance with further mobility increase for values up to 28 $cm^2/V\,s$. For comparison, arrows indicating the reported carrier mobility values of CMTS and its sister compound CMTSe were added to Fig. 5. These arrows highlight a comparison between the charge transport properties of the two materials. CMTSe exhibits an electron/hole mobility of 16 $cm^2/V\,s$ and possesses physical properties similar to those of CMTS [42]. This comparison suggests that both compounds are likely to display comparable photodetection performance, supporting their suitability for optoelectronic applications. The relatively small impact of increased electron/hole mobility on photodetector performance is unusual, as in general, higher electron/hole mobility leads to improved photodetector performance [43]. This could be attributed to several factors, such as saturation of charge-collection efficiency, carrier recombination before they reach the electrodes, or intrinsic material properties that do not improve further with increased mobility.

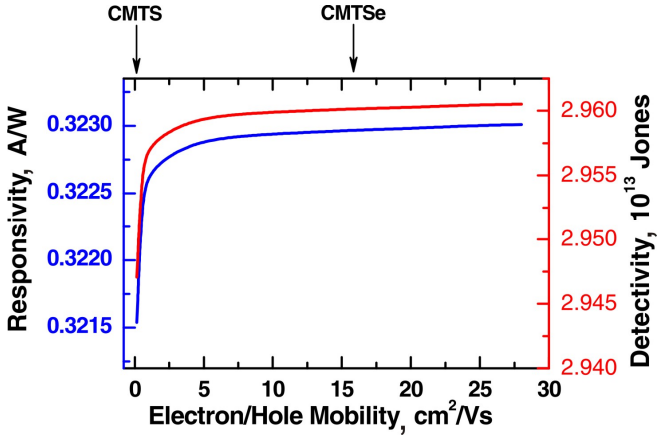

Fig. 5. Influence of the CMTS electron/hole mobility variation on the photodetector's responsivity (left) and detectivity (right). The arrows indicate the mobility values for CMTS and CMTSe (see the text).

Determining the optimal illumination wavelength for optimal photodetection performance is essential for identifying the desired practical applications. Therefore, the modelled device's sensitivity was evaluated at varying incident illumination wavelengths, as shown in Fig. 6. The device exhibits a promising broadband photoresponse across the incident spectrum, with a highly focused sensitivity in the 600–800 nm range, demonstrating peak performance at 800 nm, where the maximum detectivity is 5.17×10^{13} Jones and the peak responsivity is 0.56 A/W.

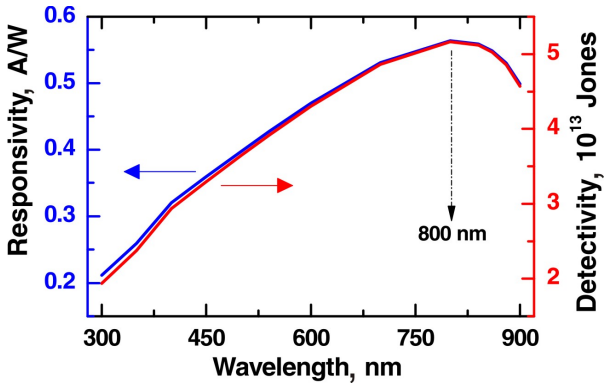

Fig. 6. Impact of irradiation wavelength on the responsivity (left) and detectivity (right) of the CMTS photodetector.

The observed dependence of detectivity and responsivity on incident wavelength is consistent with findings from several previous studies [44-46]. This significant impact of wavelength on photodetector performance parameters is attributed to variations in the material's optical properties and the corresponding photon-absorption efficiency at different wavelengths, which dictate changes in the material's absorption coefficient.

The potential of CMTS as a semiconductor absorber material for photosensing applications is further explored through recombination rate characteristics presented in Fig. 7 and by comparing the device with other materials commonly used in MSM-structured photodetectors, as detailed in Table 2. As clearly demonstrated in Fig. 7, the recombination rate inside the CMTS decreases with depth from 9.3×10^{21} cm^{-3} s^{-1} to 1.45×10^{16} cm^{-3} s^{-1}. This decrease means fewer photogenerated charge carriers are lost before they can be collected as electrical current, leading to higher performance. This output makes CMTS a candidate for future photodetector technology. Table 2 presents a critical performance comparison between the newly proposed CMTS-based photodetector and existing proposed photodetectors. The comparison indicates that utilizing CMTS as the light-harvesting layer in MSM configuration is effective for adaptation in photosensing applications.

Table 2. Comparison among different photodetectors with MSM configuration.

Photodetector	Responsivity (A/W)	Detectivity (Jones)	References
FTO/$CH_3NH_3PbI_{3-x}Cl_x$/Au	0.45	6.01×10^{11}	11
FTO/CZTS/Au	0.50	~1.00×10^{12}	25
FTO/Cs_2SnI_6/Au	0.41	3.4×10^{12}	26
FTO/CMTS/Au	0.56	5.17×10^{13}	This work

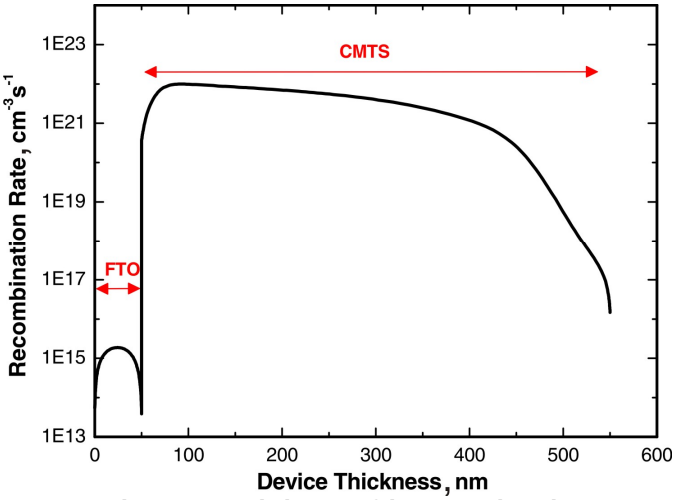

Fig. 7. Recombination rate behavior of the CMTS photodetector.

After several parameter investigations, Table 3 presents the optimal physical parameters for CMTS, which yield optimal performance for the photodetector.

Table 3. Optimal parameters for the CMTS layer.

Thickness (nm)	Doping density (cm^{-3})	Energy band gap (eV)	Carrier mobility (cm^2/Vs)
1000	1×10^{14}	1.3	16

Finally, it is important to note that further investigation using more advanced tools, such as TCAD modeling, is highly recommended and will strengthen the guide for future experimental work, given some intrinsic limitations in SCAPS-1D, such as its one-dimensional nature and simplified treatment of Schottky contacts and interface states.

4. Conclusions

In this research, a photodetector utilizing CMTS in an MSM structure is modelled and numerically analyzed using SCAPS-1D. The results reveal the device's potential for efficient photosensing applications. By optimizing parameters such as thickness, doping levels, and electron/hole mobilities in the absorber layer, we observed substantial enhancements in both responsivity and detectivity. At an incident light wavelength of 800 nm, the device achieved a responsivity of 0.56 A/W and a detectivity of 5.17×10^{13} Jones. In addition, the featured recombination rate behavior within the CMTS, in parallel with the device's excellent performance compared with other pre-investigated photodetectors, indicates that CMTS-based photodetectors, due to their simple design, are well positioned to contribute to the development of affordable photosensing solutions in the future.

Acknowledgments and Funding. The authors gratefully acknowledge Marc Burgelman from the University of Gent, Belgium, for providing free access to the SCAPS-1D software. This work was supported and funded by Abdullah Al-Salem University, Research Project No. IP-01/24.

Disclosures. The authors declare no conflicts of interest.

References

1. Marouf, H., Abdel-Salam, N., El-Rabaie, E. S. M., Rashed, A. N. Z., & ElKhamisy, K. M. (2025). A Comprehensive Review Of Photodetectors: Materials, enhancement techniques, perspectives, and recent directions. *Journal of Optics*, 1-23.
2. Chetia, A., Bera, J., Betal, A., & Sahu, S. (2022). A brief review on photodetector performance based on zero-dimensional and two-dimensional materials and their hybrid structures. *Materials Today Communications, 30*, 103224.
3. Abbas, K., Ji, P., Ullah, N., Shafique, S., Zhang, Z., Ameer, M. F., Qin, S., & Yang, S. (2024). Graphene photodetectors integrated with silicon and perovskite quantum dots. *Microsystems & Nanoengineering, 10*, 81.
4. Ren, H., Chen, J.-D., Li, Y.-Q., & Tang, J.-X. (2021). Recent progress in organic photodetectors and their applications. *Advanced Science, 8*(1), 2002418.
5. Jiao, Y., Lu, G., Feng, Y., Zhang, C., Wang, W., Wu, S., Chen, M., Ma, M., Li, W., & Yang, C. (2021). Towards high-sensitivity infrared detectors using $Cu_2Cd_xZn_{1-x}SnSe_4$ thin films by SCAPS simulation. *Solar Energy, 225*, 375–381.
6. Wang, H., Sun, Y., Chen, J., Wang, F., Han, R., Zhang, C., Kong, J., Li, L., & Yang, J. (2022). A review of perovskite-based photodetectors and their applications. *Nanomaterials, 12*, 4390.
7. Chetia, A., Saikia, D., & Sahu, S. (2022). Design and optimization of the performance of $CsPbI_3$-based vertical photodetectors using SCAPS simulation. *Optik, 269*, 169804.
8. Zou, J., Zhang, S., & Tang, X. (2024). Recent advances in organic photodetectors. *Photonics, 11*(11), 1014.
9. Yu, Y., Hu, Y., Yang, J., & Wei, Z. (2022). Recent advances in wide-spectrum photodetectors based on low-dimensional semiconductors. *Materials Today Electronics, 2*, 100013.
10. Li, S., Zhang, Y., Yang, W., Liu, H., & Fang, X. (2020). 2D perovskite $Sr_2Nb_3O_{10}$ for high-performance UV photodetectors. *Advanced Materials, 32*(7), 1905443.
11. Kaifi, M., & Gupta, S. K. (2019). Simulation of perovskite-based solar cells and photodetectors using SCAPS software. *International Journal of Engineering Research & Technology, 12*(10), 1778–1786.
12. Saidaminov, M. I., Adinolfi, V., Comin, R., Abdelhady, A. L., Peng, W., Dursun, I., Yuan, M., Hoogland, S., Sargent, E. H., & Bakr, O. M. (2015). Planar-integrated single-crystalline perovskite photodetectors. *Nature Communications, 6*, 8724.
13. Li, G., Wang, Y., Huang, L., & Sun, W. (2022). Research progress of high-sensitivity perovskite photodetectors: Noise, structure, and materials. *ACS Applied Electronic Materials, 4*(4), 1485–1505.
14. Geng, X., Wang, F., Tian, H., Feng, Q., et al. (2020). Ultrafast photodetectors by integrating perovskites directly on silicon wafers. *ACS Nano, 14*, 2860–2868.
15. Zhao, J., Zhao, L., Deng, Y., Xiao, X., Ni, Z., Xu, S., & Huang, J. (2020). Perovskite-filled membranes for flexible and large-area direct-conversion X-ray detector arrays. *Nature Photonics, 14*, 612–617.

16. Dong, Y., Gu, Y., Zou, Y., Song, J., Xu, L., Li, J., Xue, J., Li, X., & Zeng, H. (2016). Improving all-inorganic perovskite photodetectors by preferred orientation and plasmonic effects. *Small, 12*, 5622–5632.
17. Palchoudhury, S., Ramasamy, K., & Gupta, A. (2020). Multinary copper-based chalcogenide nanocrystal systems for device applications. *Nanoscale Advances, 2*, 3069–3082.
18. Cheng, X., Liu, J., Feng, J., Zhang, E., Wang, H., Liu, X., Rong, H., Xu, M., & Zhang, J. (2018). Metal@I_2–II–IV–VI_4 core–shell nanocrystals synthesized via aqueous cation exchange for efficient photoelectrochemical hydrogen generation. *Journal of Materials Chemistry A, 6*, 11898–11908.
19. Huang, S. H., Chen, C., Tay, Y. F., Chen, S., Tang, J., & Wong, L. (2022). Emerging chalcogenide thin films for solar energy harvesting devices. *Chemical Reviews, 122*(11), 10170–10265.
20. Yılmaz, S., Basol, B. M., Atasoy, Y., Polat, I., Küçükomeroglu, T., & Bacaksız, E. (2024). Enhancement of response speed of CIGS-based photodetectors by Te doping. *Sensors and Actuators A: Physical, 377*, 115691.
21. Wu, H., Ma, C., Zhang, J., et al. (2021). High-performance photodetectors with ultrahigh photoswitching ratio and fast response speed in self-powered Cu_2ZnSnS_4/CdS PN heterojunctions. *ACS Applied Electronic Materials, 3*, 4135–4143.
22. Chowdhury, T. A. (2024). SCAPS modeling of CMTS solar cells with ZrS_2 buffer layers. *Acta Physica Polonica A, 145*(4), 215–224.
23. Hassanien, A. S., & El Radaf, I. M. (2020). Optical characterization of quaternary Cu_2MnSnS_4 thin films synthesized by spray pyrolysis. *Physica B: Condensed Matter, 585*, 412110.
24. Sarilmaz, A., Ozel, F., Karabulut, A., Orak, İ., & Şahinkaya, M. A. (2020). Effects of temperature and frequency on the electrical characteristics of Cu_2MnSnS_4-based heterojunctions. *Physica B: Condensed Matter, 580*, 411821.
25. Kukreti, S., Sapkota, D. J., Ramawat, S., & Dixit, A. (2022). Near-infrared photodetector performance of Cu_2ZnSnS_4 in MSM configuration: A theoretical study. *Optik, 264*, 169385.
26. Roy, N. (2024). Investigating Cs_2SnI_6 as a promising material for high-performance self-powered broadband photodetection application. *Journal of Physics and Chemistry of Solids, 203*, 112730.
27. Burgelman, M., Nollet, P., & Degrave, S. (2000). Modelling polycrystalline semiconductor solar cells. *Thin Solid Films, 361–362*, 527–532.
28. Hossain, M. K., Toki, G. F. I., Samajdar, D. P., et al. (2023). Coupled optoelectronic and photovoltaic analysis of lead-free $CsSnI_3$ perovskite solar cells using DFT and SCAPS-1D simulations. *ACS Omega, 8*, 22466–22485.
29. Yasin, S., Christopoulos, S., Abu Waar, Z., & Moustafa, M. (2025). Numerical modeling and optimization of high-performance $CsSnI_3$ perovskite photodetectors. *Journal of Electronic Materials, 54*, 5690–5700.
30. Abu Waar, Z., Yasin, S., Christopoulos, S., & Moustafa, M. (2025). Exploring WS_2 as a potential buffer layer for improved CFTS solar cell performance. *Romanian Journal of Physics, 70*, 612.
31. Yasin, S., Abu Waar, Z., Al Zoubi, T., & Moustafa, M. (2021). Optoelectronic simulation of a high-efficiency C_2N-based solar cell via buffer layer optimization. *Optical Materials, 119*, 111364.
32. Makinudin, A., Al-Zuhairi, O., Anuar, A., Zainorin, M., Abu Bakar, A., DenBaars, S., & Supangat, A. (2021). Impact of crystallinity on the performance of semi-polar (11–22) GaN UV photodetectors. *Materials Letters, 286*, 129244.
33. Mohamad, W. F., Abou Hajar, A., & Saleh, A. N. (2006). Effects of oxide layers and metals on photoelectric and optical properties of Schottky barrier photodetectors. *Renewable Energy, 31*, 1493–1503.
34. Pansuriya, T., Malani, R., & Kheraj, V. (2022). Effect of buffer layer on CMTS-based thin-film solar cells using SCAPS-1D. *Optical Materials, 126*, 112150.
35. Isha, A., Kowsar, A., Kuddus, A., Hossain, M. K., Ali, M. H., Haque, M. D., & Rahman, M. F. (2023). High-efficiency Cu_2MnSnS_4 thin-film solar cells with SnS BSF and CdS ETL layers: A numerical simulation. *Heliyon, 9*(5), e15716.
36. Schukraft, G. E. M., Moss, B., Kafizas, A. G., & Petit, C. (2022). Effect of band bending in photoactive MOF-based heterojunctions. *ACS Applied Materials & Interfaces, 14*, 19342–19352.
37. Ouslimane, T., Et-Taya, L., Elmaimouni, L., & Benami, A. (2021). Impact of absorber layer thickness, defect density, and operating temperature on MAPbI solar cells with ZnO ETL. *Heliyon, 7*(3), e06379.
38. Manzoor, G., Sharma, K. K., & Bharti, G. K. (2023). Modeling and simulation of heterojunction-based multilayer high-speed vertical CIGS photodetectors. In *Proceedings of the International Conference for Advancement in Technology (ICONAT)* (pp. 1–4).
39. Xie, W., Du, C., Luo, Y., & Cao, S. (2025). Design and optimization of high responsivity and detectivity in lead-free tin-based perovskite photodetectors by numerical simulation. *Journal of Physics and Chemistry of Solids, 207*, 112919.
40. Myers, S., Plis, E., Khoshakhlagh, A., Kim, H. S., Sharma, Y., Dawson, R., Krishna, S., & Gin, A. (2009). Effect of absorber doping on electrical and optical properties of nBn-based type-II InAs/GaSb strained-layer superlattice infrared detectors. *Applied Physics Letters, 95*, 121110.
41. Talebi, B., & Moradi, M. (2025). Role of MoS_2 and $MoSe_2$ thin films in the performance of new-generation CMTSe solar cells. *Solar Energy, 292*, 113449.

42. Zhou, W., Ma, T., Tian, Y., Jiang, Y., & Yu, X. (2024). Dielectric-engineered graphene transistors for high-performance near-infrared photodetection. *Science, 27*(3), 109314.
43. Su, L., Zuo, Y., & Xie, J. (2021). Scalable manufacture of vertical p-GaN/n-SnO_2 heterostructures for self-powered ultraviolet photodetectors, solar cells, and dual-color LEDs. *InfoMat, 3*, 598–610.
44. Tang, Y., Jin, P., Wang, Y., Li, D., et al. (2023). Enabling low-drift flexible perovskite photodetectors by electrical modulation for wearable health monitoring and weak-light imaging. *Nature Communications, 14*, 4961.
45. Avdizhiyan, A. Y., Lavrov, S. D., Abdullaev, D. A., Shestakova, A. P., Kulyuk, L. L., & Mishina, E. D. (2021). Tunable spectral properties of photodetectors based on quaternary transition metal dichalcogenide alloys. *IEEE Sensors Journal, 21*(1), 325.
46. Shukla, R., Kumar, R. R., & Pandey, S. K. (2021). Theoretical study of charge carrier lifetime and recombination in eco-friendly perovskite solar cells. *IEEE Transactions on Electron Devices, 68*(7), 3446.

Yasin, S., Abu Waar, Z., Christopoulos, S., Moustafa M. (2026). In-Depth Numerical Evaluation and Performance Optimization of CMTS Photodetector**.** *Ukrainian Journal of Physical Optics*, *27*(2), 02058 – 002069. doi: 10.3116/16091833/Ukr.J.Phys.Opt.2026.02058

Анотація. *Фотодетектори є важливими елементами в широкому спектрі технологічних галузей, особливо для передових застосувань фоточутливості. Це дослідження представляє детальну числову оцінку та оптимізацію продуктивності шарів сульфіду міді-марганцю-олова (CMTS), зосереджуючись на функції поглинального шару у фотодетекторному пристрої. Дослідження зосереджене на аналізі впливу різних конструктивних параметрів, з акцентом на максимізацію ефективності та функціональності структури легованого фтором оксиду олова (FTO)/CMTS/Au. Комплексний чисельний аналіз фізичних властивостей поглинального шару CMTS дозволив визначити у досліджуваному діапазоні оптимальну товщину, ширину забороненої зони, концентрацію легування та електрон-діркову рухливість для підвищеної ефективності фотодетектора, які становлять відповідно 1000 нм, 1,3 еВ, 1×10^{14} $см^{-3}$ та 28 $см^{-2}/с$. Крім того, досліджено вплив довжини хвилі падаючого світла на поведінку фотодетектора. Результати показують, що пристрій демонструє оптимальну роботу при довжині хвилі падаючого випромінювання 800 нм. За цих оптимізованих значень та умов фотодетектор досягає чутливості 0,56 А/Вт та детективності $5{,}17\times10^{13}$ Джонса. Отримані результати свідчать, що запропонований пристрій є перспективним для створення економічно ефективних, технологічно простих у виготовленні та надійних фотодетекторів, що робить його дуже перспективним матеріалом для майбутніх технологій фоточутливості.*

Ключові слова: *фотодетектор, CMTS, чутливість, детективність, SCAPS.*